Proceedings of the ASME 2015 34th International Conference on Ocean, Offshore and Arctic Engineering
OMAE2015
May 31-June 5, 2015, St. John's, Newfoundland, Canada

OMAE2015-41527

EFFECT OF LAY ANGLE OF ANTI-BUCKLING TAPE ON LATERAL BUCKLING BEHAVIOR OF TENSILE ARMORS

Chongyao Zhou
MARINTEK
7450 Trondheim,
Norway

Svein Sævik
NTNU
7491 Trondheim,
Norway

Naiquan Ye
MARINTEK
7450 Trondheim,
Norway

Guomin Ji
MARINTEK
7450 Trondheim,
Norway

ABSTRACT

During deep water flexible pipe installation, the pipe is normally free hanging in empty condition from the installation vessel to the seabed. This will introduce large hydrostatic forces to the pipe causing true wall compression. In addition, the pipe will be exposed to cyclic bending caused by waves and vessel motion. The combination of true wall axial compression and cyclic bending may lead to tensile armor instability in both lateral and radial directions. If the anti-buckling tape is assumed to be strong enough, the inner tensile armor will lose its lateral stability first due to the gap that may occur between the inner tensile armor and the pipe core, hence restricting the available friction restraint forces. These may further be reduced by cyclic motions that act to create slip between the layers, hence introducing lateral buckling of the tensile armor, with associated severe global torsion deformation of the pipe, ultimately causing the pipe to lose its integrity.

The anti-buckling tape is designed to prevent the radial buckling behavior, however, its effect on lateral buckling has not yet been documented in available literature. In the present paper, the effect of the winding direction of the anti-buckling tape on the twist of the cross section is studied, including comparisons with available test data from literature.

1 INTRODUCTION

The tensile armor is a key functional component of flexible pipes providing resistance to gravity load and cyclic bending caused by environmental loads. It normally consists of an even number of layers which are cross wounded by a number of flat rectangular wires with a lay angle of 30 to 55 degrees. For deep water applications, the coupled effect from cyclic bending and external pressure may lead to lateral and radial buckling of tensile armors during pipe installation and operation.

Any failure of the tensile armor wires may cause lose of the pipe integrity and is therefore not permitted by design standards. Ultimate and fatigue strength have been extensively studied in recent years, while quite little effort has been devoted to address the mechanism of the lateral and radial buckling of the tensile armor wires. Figure 1 illustrates two types of tensile armor buckling scenarios: the radial buckling and lateral buckling. It can be seen that the integrity of the flexible pipe may be completely destroyed once these failure modes occur.

Radial buckling Lateral buckling

FIGURE 1 BUCKLING FAILURE MODES [3]

Anti-buckling tape is usually used to prevent radial buckling of tensile armor, however it will also prevent lateral buckling. In order to study the mechanisms of lateral buckling of tensile armor and the effect of anti-buckling tape, experiments were carried out for three risers with different size and material under same load conditions in 2012 [1]. Lateral buckling was

first introduced and described by Braga and Kaleff [2] based on experimental results. Further experiments to study the lateral buckling behavior were carried out by Secher, Bectare and Felix-Henry, studying flexible pipe behavior at 3000m water depth [3], however, details were not available in literature.

Lateral buckling behavior due to the cyclic bending was studied by Østergaard, Lyckegaard and Andreasen [4]. The work included both experimental tests and formulation of a theoretical model under the assumption of no friction [5]-[6].

In the present work, the effect of friction is included and the focus is on the effect of anti-buckling tape with respect to the lateral failure mode.

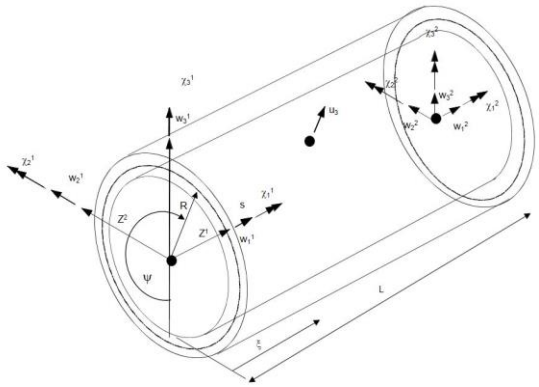

FIGURE 2 HSHEAR363 ELEMENT

2 THEORETICAL BACKGROUND

2.1 Theoretical model

The axial stress represents the primary component in the tensile armor, providing structural strength in the axial direction (tension and end cap). The primary stresses are mainly caused by axisymmetric loads, including tension, torsion, internal and external pressure loads. In addition secondary stresses will occur due to local bending and friction due to bending.

Curved beam theory can be used for the tensile armor wire which is a long and thin slender structure. The theoretical model applied here has already been presented elsewhere by the Sævik, Thorsen and Li, [7], [9], including tensile armor and core contact elements (HSHEAR353 and HCONT353). However, since then a few more elements have been developed. These are:

- The HSHEAR363 element that enables to model the tape, pressure spiral and sheath layers
- The HCONT363 element that enables to model contact between the tensile armor and the tape, sheath and pressure spiral layers.

The HSHEAR363 is a 13 degree of freedom (DOF) beam element which includes the standard 12 beam DOF's and one extra to capture radial motion, see Figure 2. The element applies thin shell theory for the sheath, whereas the longitudinal helix strain is used for the armor wire. In both cases, the strain is expressed in terms of the radial DOF and the beam axial strain and torsion quantities. It is noted that this represents a simplification that excludes considering the 3D stress state, however, this is justified by axial membrane action being the primary variable in this case.

The HCONT363_element provides contact to the tensile armor as shown in Figure 3.

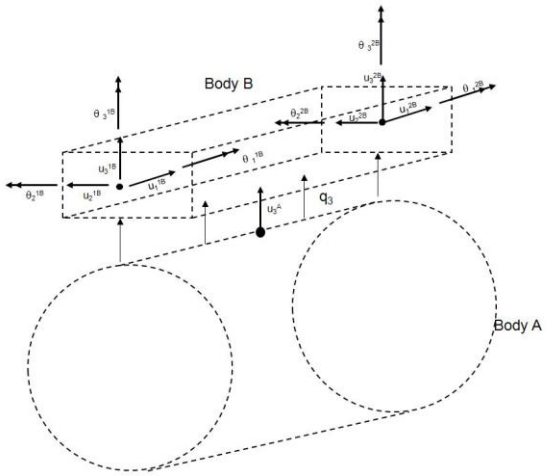

FIGURE 3 HCONT363 ELEMENT

The longitudinal stress of tensile armor wire and anti-buckling tape wire is mainly studied. The definition of longitudinal stress σ_{xx} is shown in Figure 4, which is the same in tensile wire element and anti-buckling tape element.

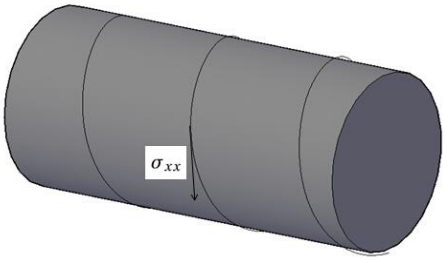

FIGURE 4 DEFINITION OF σ_{xx}

2.2 Failure Mechanism

The process of the lateral buckling is initiated from the end cap force, where the two tensile layers will be squeezed against the anti-buckling tape and a gap will be developed

between the inner tensile armor layer and the pressure armor. Assuming the anti-buckling tape is strong enough, the tensile layer will only be able to slide in the lateral direction. The inner tensile armor layer will have the smallest resistant friction force and begin to lose its capacity first. In order to keep the torsion balance in the cross-section, a loss in axial compression is necessary for the outer layer associated with pipe twist.

Then the pipe will rotate following the lay angle direction of the first tensile layer. If the pipe is suffering a cycle loading, a certain rotation will take place during each cycle until the failure of the cross-section reaches.

2.3 Analytical Method

If a harmonic buckling shape is assumed, the buckling load for the model shown in Figure 5 is calculated as the Euler buckling load:

$$P = \frac{\pi^2 EI}{l_e^2} \tag{7}$$

where l_e is the buckling length which is influenced by the boundary conditions, which is the length of the bar in this case.

FIGURE 5 BUCKLING MODEL

For the lateral buckling problem of the flexible pipe, the situation is more complex because any lateral motion is associated with changes in bending and twist of the wire. Under the assumption of no friction, a conservative estimate of the axial buckling force contribution from each wire can be achieved from the curve beam differential equation [11]:

$$P = \cos\alpha[\frac{\pi^2 EI_3}{l^2} + GI_1(\kappa_2^2 - \kappa_t\kappa_2) + 4EI_2\kappa_1^2 + EI_3\kappa_1^2] \tag{8}$$

where E is the Young's modulus, and G is the shear modulus.

κ_1, κ_2 are the initial torsion and normal curvature and κ_t is the cylinder curvature in tendon transverse direction, which can be expressed as:

$$\kappa_1 = \frac{\sin\alpha\cos\alpha}{R} \tag{9}$$

$$\kappa_2 = \frac{\sin^2\alpha}{R} \tag{10}$$

$$\kappa_t = \frac{\cos^2\alpha}{R} \tag{11}$$

The inertial moments corresponding to the three axis are listed below, where *b* is the width of the tendon cross-section and *t* is the thickness.

$$I_1 = \frac{1}{3}bt^3 \tag{12}$$

$$I_2 = \frac{1}{12}bt^3 \tag{13}$$

$$I_3 = \frac{1}{12}tb^3 \tag{14}$$

In this formulation, as l is very large, the first term will be very small and can be neglected, so the formula can be rewritten to:

$$P = \cos\alpha[GI_1(\kappa_2^2 - \kappa_t\kappa_2) + 4EI_2\kappa_1^2 + EI_3\kappa_1^2] \tag{15}$$

It is a function of the tensile layer radius, lay angle and the thickness and width of the tendon cross-section. The buckling force will be reduced as a function of R and α. These parameters are shown in Figure 6.

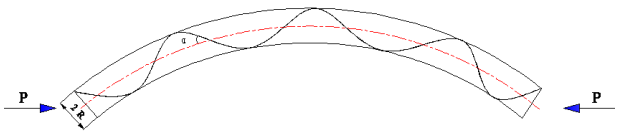

FIGURE 6 TENSILE LAYER RADIUS AND LAY ANGLE

The basic model in test is shown in Figure 7 and the relative strain-force curve is shown in Figure 8

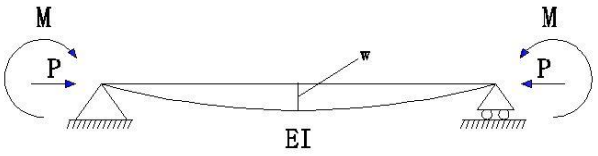

FIGURE 7 BUCKLING MODEL

It should be noticed in Figure 8 that the buckling load is divided into two types, one is termed as buckling load and another is post-buckling load. The first peak is due to the imperfection in the tendon, which means this part will snap. It should be noticed that the buckling load is the result calculated from the formula (15). σ_y is yield stress, A is cross-section area and P is the yield load of the tendon.

The post-buckling load happens in the region which is determined by the elastic-plastic behavior of the material. It is the largest load which the tensile can withstand once the buckling occurs.

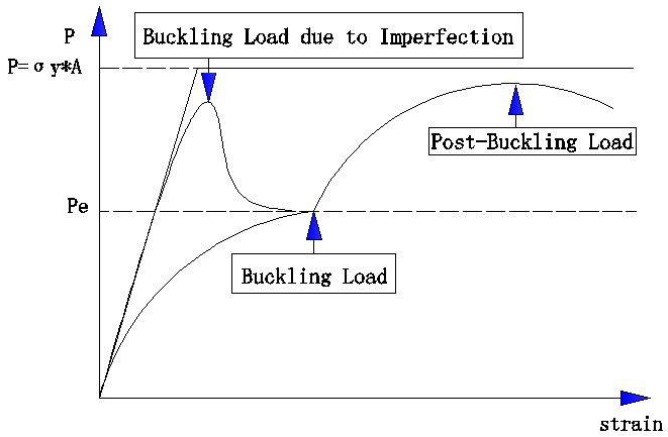

FIGURE 8 STRAIN-FORCE CURVE OF BUCKLING

3 ANALYSIS TOOLS

Analysis of the flexible riser cross section has been performed by using the finite element software BFLEX which is developed by MARINTEK. BFLEX is based on the principle of virtual displacement and a Co-rotational formulation is applied to solve the non-linear equilibrium equations. In the analysis of tendon bending, the loxodromic curve elastic bending theory is used neglecting the transverse slip based on the work by Sævik [9]-[10].

The first release of the software was made in 1990s for stress and fatigue analysis of tensile armor wire in the flexible risers. It has been under continuous development since then by adding new functionalities to meet the emerging requirements for deep water application of flexible risers where the latest ones are the introduction of the HSHEAR363 and HCONT363 element types which are developed with aims to handle the lateral buckling of the tensile armors as presented in this paper.

4 MODEL DESCRIPTION

The flexible pipe studied in the paper is based on a full scale test carried out by Østergaard in 2012 [1]. Tests were carried out for three flexible risers with the inner diameter of 6 inch, 8 inch and 14 inch. The detail information is listed in Table 1 [1].

TABLE 1 PIPES DESIGN AND MATERIAL PROPERTIES[1]

Pipe layer/Pipe design		6" Riser*1	8" Riser*2	14" Jumper*2
Inner layer of tensile armor wires	Outer diameter(m)	0.201	0.276	0.442
	Pitch length, L_{pitch}(m)	1.263	1.474	2.247
	Pitch angle, φ_{hel}(deg)	26.2	30	31.5
	Wire size(height*width)(mm)	3 x 10	5 x 12.5	4 x 15
	Number of wires	52	54	70
Outer layer of tensile armor wires	Outer diameter(m)	0.209	0.289	0.452
	Pitch length, L_{pitch}(m)	1.318	1.525	2.345
	Pitch angle, φ_{hel}(deg)	-26.2	-30.3	-31.0
	Wire size(height*width)(mm)	3 x 10	5 x 12.5	4 x 15
	Number of wires	54	56	72
High strength anti-birdcaging tape*3	Outer diameter(m)	0.212	0.292	0.455
	Pitch length, L_{pitch}(m)	0.075	0.025	0.140
	Pitch angle, φ_{hel}(deg)	83.5	88.4	-84.4
	Tape size(height*width)(mm)	1 x 60	1.8 x 1.3	1 x 60
	Number of wires	1	8	2
Outer sheath*4	Outer diameter(m)	0.225	0.434	0.477
	Thickness(mm)	6.0	10.0	10.0
	Number of inner layer pitches in pipe sample (including end-fitting)	3.96	3.39	3.34

*1) A basic grade steel used for wires with yield strength of approximately 650 Map, elastic modulus 210 GPa, Poison's ratio 0.3

*2) A high strength grade steel used for wires with yield strength of approximately 1350MPa, elastic modulus 210GPa, Poison's ratio 0.3

*3) Tape material properties chosen are: elastic modulus 27GPa. Poison's ratio 0.4

*4) Sheath material properties chosen are: elastic modulus 400MPa, Poison's ratio 0.4

The full model shown in Figure 9 includes two cores, two tensile layers, one structural tape layer between the two tensile layers, one anti-buckling layer and one sheath layer. One core is modeled by elastic pipe element which is used specially for the loading condition. The other core is used to support the inner tensile layer and is modeled by the element helix element. The inner and outer tensile layers are also built by helix element. Each tensile layer is represented by four helix tendons. The structural tape, anti-buckling tape and the sheath are modeled by the HELIX363 element. The friction between the layers is included and calculated from the contact element which is modeled by HCONT363 contact element, see [12] and [13]. Since the contact between the anti-buckling tape and the sheath will not influence a lot, the two elements are merged into the same node system, which means there will only be four contact layers for contacting the two tensile layers. The cross section is shown in Figure 10. The friction coefficient between the layers is set to be 0.15.

There are two loads applied on the model: cyclic bending around the global Y-axis and compression along the global X-axis as shown in Figure 7. The analysis of the first 10 seconds is static analysis, and the next 2460 seconds is dynamic analysis to ensure numerical stability. Firstly, the positive axial strain along local X-axis is added to the small pipe from 0^{th} second to 10^{th} second with one load step to establish axial compression. Then the prescribed curvature around Y-axis is applied from 10^{th} second to 2460^{th} second, representing by a ramping function from zero to the specified curvature based on the data sheet and then back to zero. The ramping function adopted in BFLEX is a harmonic function.

Each bending cycle lasts 20 seconds and time increment is 0.005s in dynamic analysis, which is necessary to ensure

numerical stability. This loading process is based on the realistic operation behavior of riser in deep water application. The compression at the two ends of riser is end-cap force and the cyclic bending is mainly due to hydrodynamic load and vessel motion.

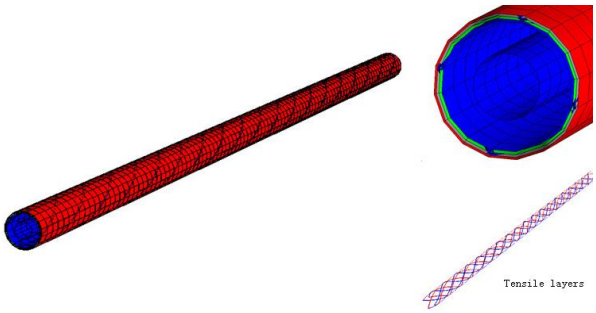

FIGURE 9 MODEL IN BFLEX

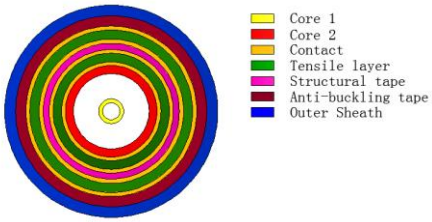

FIGURE 10 MODEL CROSS SECTION

5 ANALYSIS AND RESULTS

5.1 Cases Overview

Twelve cases are carried out to study the lateral buckling behavior due to cyclic bending which is consistent to the experimental input data sheet as shown in Table 1 and the loading conditions for the 12 cases are shown in Table 2.

The pipe length is five times of the pitch length of the tensile armor layer. The effect of the stiffness on the buckling mechanism will be discussed later.

TABLE 2 LOADING CONDITIONS

Pipe ID	Case number	Applied compression (kN)	Bending radius (m)
6 inch riser, L=6.315m	2	265	11
	3	80	11
	4	210	11
	5	160	11
	6	265	8
14 inch jumper, L=11.235m	7	277	21
	8	269	8
	9	411	10
	10	950	12
8 inch riser, L=7.370m	11	300	12
	12	400	12
	13	700	12

5.2 Analysis Process

The criterion of failure is when the steel loses its capacity, i.e. the yield strength of the material is reached. For the 6 inch riser, the wires are made of basic grade steel with the yield strength of approximately 650Mpa. For the 8 inch riser and 14 inch jumper, the wires are made by high strength grade steel with the yield strength of approximately 1350Mpa. If there are no failures, the rotation will be very small and increase slowly.

Case 1 is studied as an example for the process which is shown in Figure 11. To avoid the influence of the boundary conditions, the middle part of the pipe is isolated for the investigation. The red part of the tendon indicates the elements where the steel yield stress is exceeded.

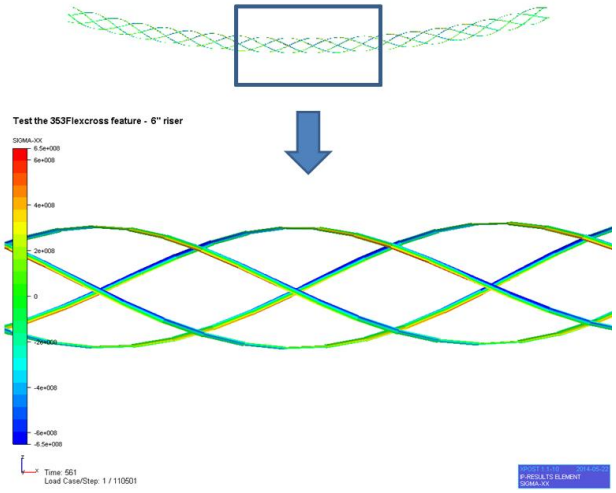

FIGURE 11 EXAMPLE OF FAILURE MODE STUDY PROCESS 1

After that, the moment (load step) at which the exceeding of the yield strength (red color) occurs will be selected to find the corresponding end rotation, which is shown in Figure 12. Since the inner tensile layer fails at first, in order to keep the torsion balance, the outer tensile layer will rotate following the direction of outer layer lay angle which results in the rotation of the whole pipe. For the tested pipes, the lay angle is negative, so the end rotation will be negative as well as described earlier in the paper.

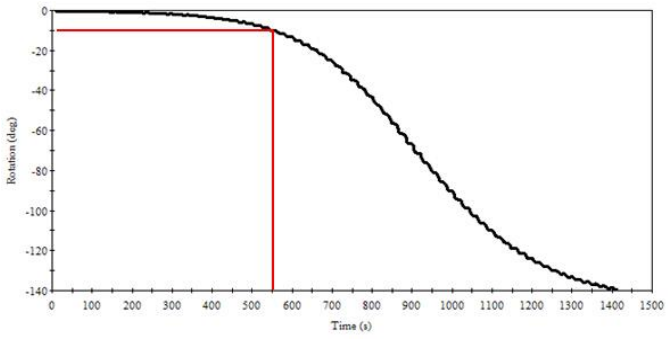

FIGURE 12 EXAMPLE OF FAILURE MODE STUDY PROCESS 2

Figure 13 demonstrates the longitudinal stress as a function of time for one critical element. It shows the history when the yield stress of 650MPa is exceeded.

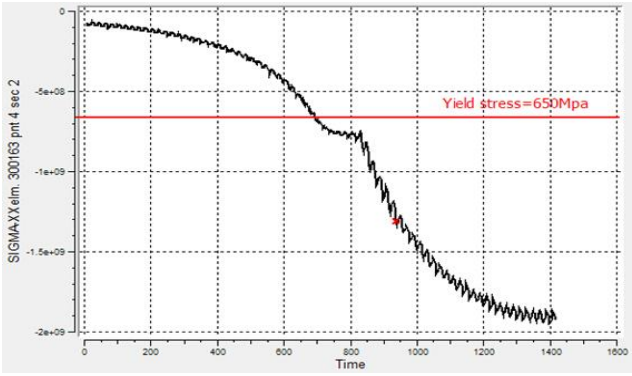

FIGURE 13 LONGITUDINAL STRESS σ_{xx}, CASE 2

In addition, case 3 is studied as no failure case as shown in Figure 14 below. The stress in tendon does not exceed the yield stress of the steel, thus the rotation is very small and buckling will not happen.

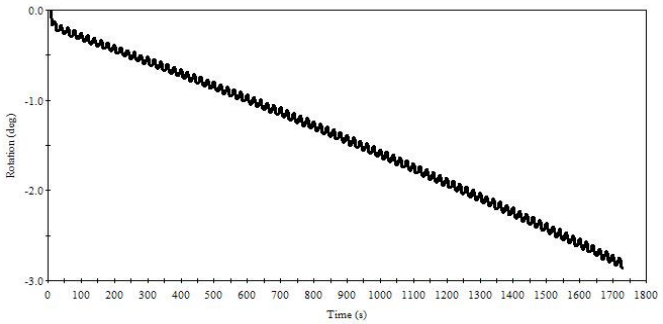

FIGURE 14 EXAMPLE OF STABLE CASE, CASE 3

Then the element with the maximum longitudinal stress is picked out as shown in Figure 15. The longitudinal stress does not exceed the yield stress of 650MPa, which means there is no failure in the tensile layer during the cyclic bending.

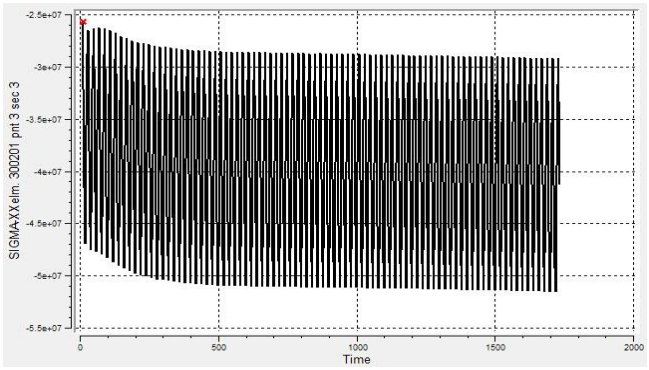

FIGURE 15 LONGITUDINAL STRESS σ_{xx}, CASE 3

5.3 Results of End Rotation

The comparison of end rotation and failure/no failure between BFLEX simulation and measured values are shown in Table 3.

TABLE 3 RESULTS OF PIPE FAILURE DUE TO CYCLIC BENDING

Pipe ID	Case number	Applied compression (kN)	Bending radius (m)	Results in experiment	Pipe twist before unloading (deg)	Results in Bflex2010	Pipe twist before failure (deg)
6 inch	2	265	11	Failure	45 (increasing)	Failure	10 (increasing)
	3	80	11	No failure	<1 (stable)	No failure	3 (slowly increasing)
	4	210	11	Failure	45 (increasing)	Failure	11 (increasing)
	5	160	11	No failure	3 (slowly increasing)	Failure	3 (increasing)
	6	265	9	Failure	45 (slowly increasing)	Failure	10 (increasing)
14 inch	7	277	21	No failure	<1 (stable)	No failure	5 (slowly increasing)
	8	269	8	No failure	6.5 (increasing)	Failure	17 (increasing)
	9	411	10	Failure	27	Failure	27 (rapidly increasing)
	10	950	12	Failure	10 (rapily increasing)	Failure	11 (rapidly increasing)
8 inch	11	700	12	Failure	27 (slowly increasing)	Failure	21 (increasing)
	12	300	12	No failure	1	No failure	2.8 (slowly increasing)
	13	400	12	No failure	15 (slowly increasing)	Failure	18 (increasing)

For the 6 inch riser, BFLEX predicts failure for Case 5 whereas no failure was observed in the test. However, for case 4 with 50 kN more compression, failure is obtained both numerically and experimentally. This indicates some conservatism in the model.

For the 14 inch jumper, the end rotations of the failure cases agree with the experimental results quite well. However, the collapse of case 8 is not obtained in BFLEX simulation, thus confirming some conservatism for this model as well.

For the 8 inch riser, the yield stress of wires is same as the 14 inch jumper. The results of failure case 11 fit well with the experimental results. However, the test case 12 which is between the failure case and no failure case is unstable and the end rotation is increasing. While the experimental result of case 12 is also unstable and the end rotation is increasing slowly, it is difficult to judge whether the pipe will eventually fail or not. This also applies for case 13, where BFLEX predicts failure whereas no failure was observed in the test.

In all cases the numerical model demonstrated some conservatism with respect to the failure criterion applied.

6 EFFECT OF ANTI-BUCKLING TAPE

The effect of the anti-buckling tape on the lateral buckling behavior of the tensile armor was studied including sensitivity analysis of the effect of the lay direction, lay angle of anti-buckling tape, and the friction coefficient between layers.

6.1 Influence of Anti-buckling Tape

The effect of anti-buckling tape was studied by comparing a case without anti-buckling tape to the case with tape. The results are shown in Figure 16, which reveals clearly the important effect of anti-buckling tape on the lateral buckling behavior. It clearly indicates that the anti-buckling tape can slow down the buckling process significantly. By simply linearizing the curves in the figure, the slope of the pipe

without anti-buckling tape is almost 20 times higher than the case with anti-buckling tape.

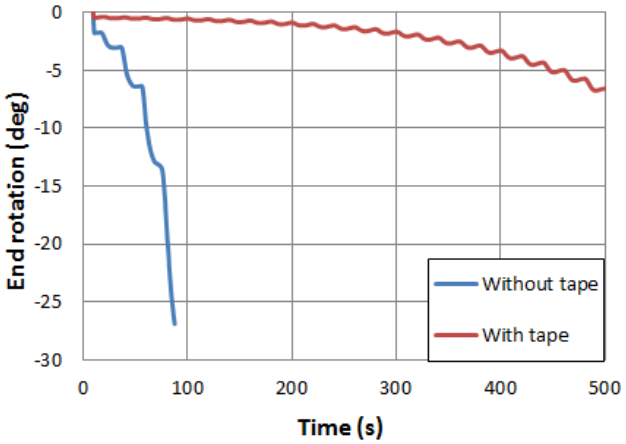

FIGURE 16 COMPARISON BETWEEN THE RISER WITH AND WITHOUT ANTI-BUCKLING TAPE

6.2 Influence of Lay Direction of Anti-buckling Tape

The anti-buckling tape is helically wounded often with a steep angle close to 90 degree, its lay angle may have influence in the buckling behavior of the tensile armors. Sensitivity study based on case 8 is hence performed to study this effect. The direction of the lay angle of anti-buckling tape in case 8 is changed from -84.4 to +84.4.

Figure 17 shows the effect of lay direction on the end rotation of the cross section. Since the lay angle of the outer tensile layer is negative, the negative anti-buckling tape lay angle means that it is in the same direction as the outer tensile layer. Whereas the positive lay angle means that it is in the opposite direction to the outer tensile layer.

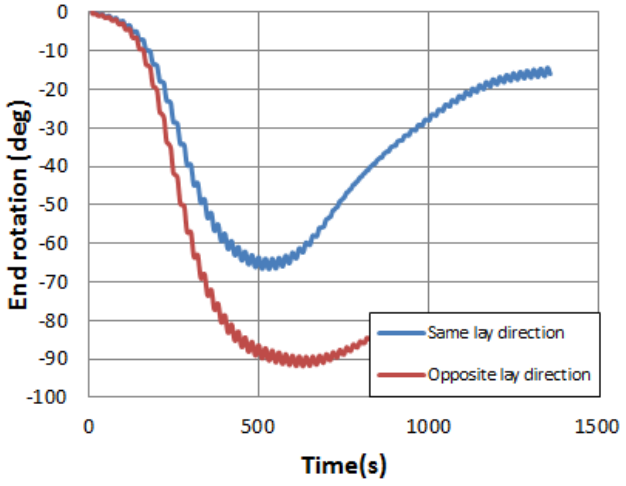

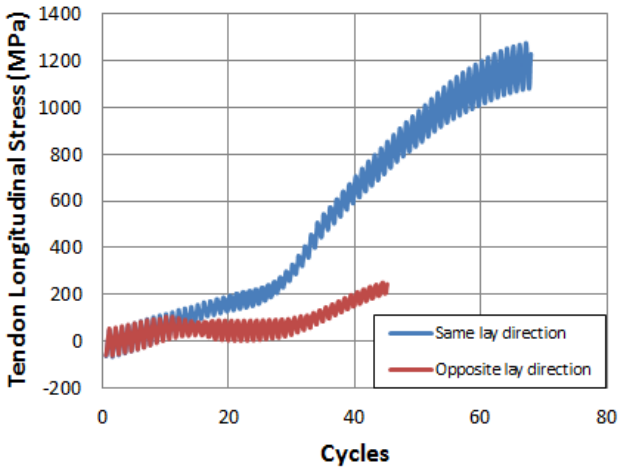

FIGURE 17 INFLUENCE OF LAY DIRECTION OF ANTI-BUCKLING TAPE

It can be seen that the negative lay angle direction will significantly affect buckling process. The results show the same direction between the outer tensile layer and anti-buckling tape will slow down the buckling process. In addition, for the same lay direction case, after the failure, the inner and outer tensile layer will lose its capacity, and then the pipe will twist back, which shows clearly the anti-buckling tape with this lay angle direction will contribute a lot to prevent the end rotation. Tensile armor in the pipe with same lay direction, will also provide more stress capacity than that with opposite lay direction, which failed at early stage.

Figure 18 shows clearly that the anti-buckling tape will bear the longitudinal stress which will also contribute to slow down the buckling process to a great extent. The longitudinal stress for both cases is shown as a function of time in Figure 19.

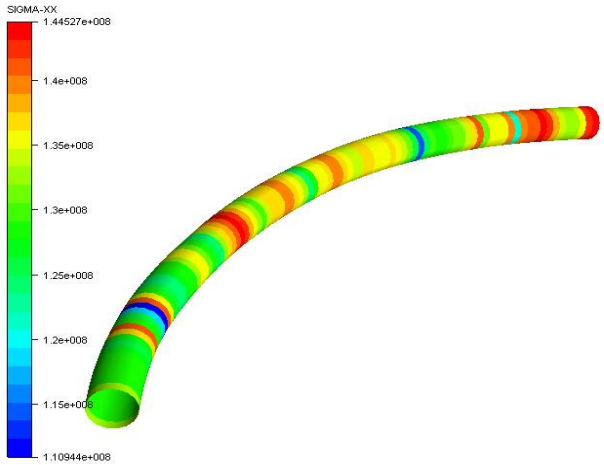

FIGURE 18 σ_{xx} IN ANTI-BUCKLING TAPE

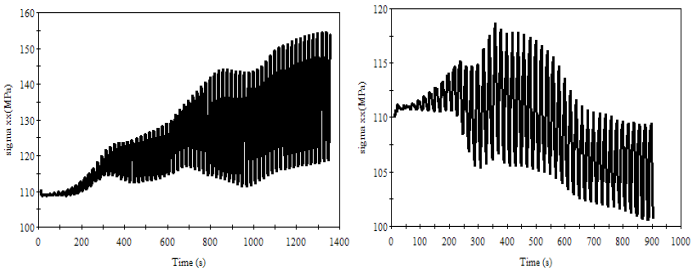

Same lay direction Opposite lay direction

FIGURE 19 LONGITUDINAL STRESS IN ANTI-BUCKLING TAPE COMPARISON BY CHANGING LAY DIRECTION

The anti-buckling tape with the same lay direction as outer tensile layer will slow down the buckling process. Furthermore, the capacity of restricting the buckling increases during cyclic bending which can stop the end rotation and make the pipe twist to the normal position. However, the tape with opposite lay direction will keep losing its restraint ability.

The reason is when the inner tensile layer loses its capacity, the outer tensile layer will try to squeeze and twist in the direction of its own lay angle. Since the anti-buckling tape has the same lay direction as the outer tensile layer, the tape will also rotate towards this direction which will make the tape to squeeze tightly onto the layer below. Thus, this rotation behavior will shorten the distance between the adjacent pitches and increase the corresponding compression, which will contribute more to the pipe to prevent end rotation.

If the lay direction of the outer tensile layer and anti-buckling tape is opposite, the tape will also rotate and follow the outer tensile layer, but the tape will become loose and keep losing its restraint ability.

6.3 Influence of Lay Angle of Anti-buckling Tape

The lay angle of anti-buckling tape may have influence in the magnitude of the end rotation. Lay angle is changed from -76 to -88 degree and the comparison is shown in Figure 20.

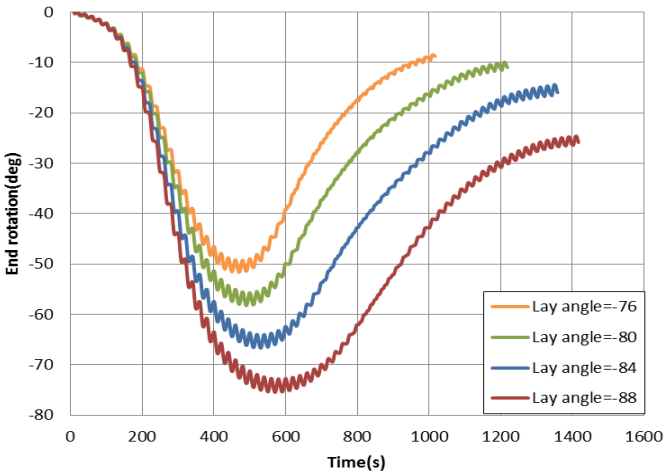

FIGURE 20 INFLUENCE OF LAY ANGLE OF ANTI-BUCKLING TAPE

Anti-buckling tape with smaller lay angle will have a better capability to prevent the end rotation. The compontent of longitudinal stress on the global x-axis direction is larger due to the smaller lay angle, which will provide more resistance when the tape is screwed closer onto pipe due to the end rotation behavior.

6.4 Influence of friction coefficient

In order to study the effect of the firction coefficient on the end rotation during cyclic bending, the friction coefficient between all the layers is changed from 0.15 to 0.2 and the results are shown in Figure 21.

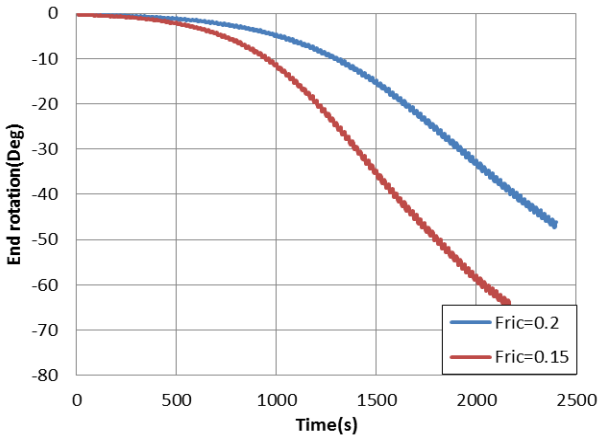

FIGURE 21 INFLUENCE OF FRICTION COEFFICIENT

Larger friction coefficient will provide more friction resistance between layers and try to stop the slip of two tensile armors during the lateral buckling process, which results in a smaller end rotation.

7 CONCLUSIONS

The following conclusions can be drawn from the above investigation:

- Couple effect between tension and cyclic bending during pipe installation and operation will lead to end rotation.
- End rotation predicted by BFLEX agrees well with most of the measured values from laboratory tests.
- In all cases the proposed failure criterion based on exceeding the yield stress demonstrated conservatism with regard to the tests
- Anti-buckling tape will have a great influence on the lateral buckling process.
- Same lay direction between the outer tensile layer and anti-buckling tape will have better performance than opposite lay direction. It has the effect to resist end rotation and the longitudinal stress carried by the anti-buckling tape will keep on increasing, specifically to inverse the end twist of the pipe.

- Smaller lay angle will have better performance than higher lay angle.
- Larger friction coefficient between layers will result in smaller end rotation.

It is important to notice that the end rotation phenomenon studied here is based on the assumption that the anti-buckling tape is strong enough and tensile layer has only one way to go which will result in lateral buckling. The radial buckling is assumed not to occur. However, the fact is that if both buckling modes are considered, the design of anti-buckling tape should also take both of modes into account. Smaller lay angle of anti-buckling tape will provide more resistance to lateral buckling, however, the radial buckling capacity will be reduced. So it is necessary to consider all these effects for an optimized design.

NOMENCLATURE

n	number of tensile armor wires
L_p	pitch length of the tensile armor wire
l_e	buckling length
l	pipe length
ε	gap between adjacent tensile armor wires
b	width of tensile armor wire
α	lay angle of the tensile armor wire
R	mean radius of the tensile armor layer
Ψ	angular coordinate starting from the lower side of the pipe
I_i	moment inertia respect to three axial
β_2	the global curvature at the cross-section center
β_{2c}	the critical global curvature with maximum shear force in the tensile wire
ω_{ip}	dynamic bending, torsion and curvature component of the wire for i=1,2,3 respectively
κ_1	initial torsion
κ_2	normal curvature
κ_3	transverse curvature
κt	cylinder curvature in tendon transverse direction
σ_{xx}	longitudinal stress in wire
u_1	longitudinal relative displacement
u_{1p}	longitudinal relative displacement by plane remain plane assumption
P	buckling load
b	width of the tendon
t	thickness of the tape layer
G	shear modulus
E	Young's modulus of the material

REFERENCES

[1] Niels Højen Østergaard. *On lateral buckling of armoring wires in flexible pipes*. PhD thesis, Aalborg University/NKT-Flexibles, Aalborg East, Denmark, 2012.

[2] M.P. Braga and P Kaleff. Flexible pipe sensitivity to bird-caging and armor wire lateral buckling. Proceedings of OMAE, 2004.

[3] P. Secher, F. Bectarte, and A. Felix-Henry. Lateral buckling of armor wires in flexible pipes: researching 3000m water depth. Proceedings of OMAE, 2011.

[4] N.H. Østergaard, A. Lyckegaard, and J. Andreasen. Simplified approaches to modeling of lateral wire buckling in the tensile armor of flexible pipes. Proceedings of OMAE, 2012.

[5] N.H. Østergaard, A. Lyckegaard, and J. Andreasen. On lateral buckling failure of armor wires in flexible pipes. Proceedings of OMAE, 2011.

[6] N.H. Østergaard, A. Lyckegaard, and J. Andreasen. A method for prediction of the equilibrium state of a long and slender wire on a frictionless toroid applied for analysis of flexible pipe structures. Engineering Structures, Vol. 34, pp. 391-399,2012.

[7] Sævik, S., Theoretical and experimental studies of stresses in flexible pipes, Computers and Structures 89(2011), pp. 2273-2291.

[8] Chongyao, Zhou; Sævik, S; Naiquan Ye. Effect of anti-wear tape on behavior of flexible risers

[9] Sævik, S., Thorsen, M.J.: Techniques for predicting tensile armor buckling and fatigue in deep water flexible pipes, Proceedings of the 31th International Conference on Ocean, Offshore and Arctic Engineering, Brazil.

[10] Sævik, S., Li, H., Shear interaction and transverse buckling of tensile armors in flexible pipes, Proceeding of the 32th International Conference on Ocean, Offshore and Arctic Engineering, 2013, Nantes, France.

[11] Sævik. S. and Guomin Ji. Differential equation for evaluation transverse buckling behavior of tensile armor wires. Proceedings of OMAE, 2014.

[12] Sævik. S. BFLEX2010 – *Theory Manual*. MARINTEK, Trondheim, Norway, 2010

[13] Sævik. S. PhD Thesis, *On Stresses and Fatigue in Flexible Pipes*, NTH, 1992.